Inorg. Chem. **2006**, *45*, 10115–10125

Lanthanide–Transition Metal Carbonyl Complexes: Condensation of Solvent-Separated Ion-Pair Compounds into Extended Structures

Pavel V. Poplaukhin, Xuenian Chen, Edward A. Meyers, and Sheldon G. Shore*

Department of Chemistry, The Ohio State University, Columbus, Ohio 43210

Received May 4, 2006

New solvent-separated ion-pair compounds and extended structures containing ytterbium(II)–transition metal isocarbonyl linkages were synthesized. $[Yb(THF)_6][M(CO)_5]_2$ (**1**, M = Mn; **2**, M = Re) were prepared via transmetalation reactions between Yb metal and $Hg[M(CO)_5]_2$ in THF. Reflux of **1** in Et_2O afforded $\{Yb(THF)_2(Et_2O)_2[(\mu\text{-}CO)_2Mn(CO)_3]_2\}_\infty$ (**3**) which is a sheet-layer structure. In ether solution, **3** is converted to $\{Yb(THF)_4[(\mu\text{-}CO)_2Mn(CO)_3]_2\}_\infty$ (**4**) which has a linear structure. In both **3** and **4**, ytterbium is 8-coordinated (distorted square antiprism geometry), four coordination sites occupied by molecules of solvent and four more by oxygen atoms of isocarbonyl linkages. The $[Mn(CO)_5]^-$ anion has trigonal bipyramidal geometry and is linked to ytterbium through two equatorial carbonyls. The formation of two minor products, $(THF)_2Mn_3(CO)_{10}$ (**5**) and $[(THF)_5Yb(\mu\text{-}CO)Mn_3(CO)_{13}][Mn_3(CO)_{14}]$ (**6**), was observed during condensation of **1** into **3** and **4**.

Introduction

The past three decades witnessed an increase of the interest in lanthanide−transition metal (Ln−M) complexes. Apart from fundamental research interest, such bimetallic arrangements promise new and exciting opportunities for practical applications in the fields of materials science[1] and catalysis.[2,3] In particular, systems containing isocyanide or isocarbonyl linkages between the lanthanide and the transition metal offer a wide variety of structural possibilities that still want exploration. Isocyanide-containing Ln−M systems proved to be precursors for superior reduced bimetallic heterogeneous catalysts for such important processes as aqueous vapor-phase hydrogenation of phenol[3b] and hydrodechlorination of chlorobenzenes.[3c,d] These catalysts have demonstrated improved activity and selectivity over the ones containing only the transition metal. The reason for such improved characteristics is believed to rest in the close interaction between the reduced lanthanide and the transition metals produced from the mixed Ln−M precursors. The polymeric framework of the precursor allows the uniform distribution of the metals over a catalyst's support surface.[3a] When the precursor is reduced to bimetallic nanoparticles, the more electropositive lanthanide can enhance the reducing properties of the transition metal by transferring electron density to the latter. The introduction of such catalysts could be useful both industrially and environmentally, since chlorobenzenes, as well as phenol, are large-scale industrial toxins. The improved selectivity of the mixed Ln−M catalysts is also very advantageous for the process of conversion of phenol to cyclohexanone, because cyclohexanone is used to prepare caprolactam, a starting material in the preparation of nylon 6.

Ln−M complexes with isocarbonyl linkages also offer a rich variety of structural combinations with the potential for a wealth of applications. We believe that they could be employed as sources for the preparation of perovskite-type oxides, $LnMO_3$, that are used as methane oxidation catalysts.[4] It is also worth noting that the synthesis and characterization of such new types of heterometallic systems have made contributions to the realm of fundamental science, improving our knowledge of how lanthanides and transition metals can

* To whom correspondence should be addressed. E-mail: shore@chemistry.ohio-state.edu.

(1) (a) Traversa, E.; Matsushima, S.; Okada, G.; Sadaoka, Y.; Sakai, Y.; Watanabe, K. *Sens. Actuators, B* **1995**, *25*, 661. (b) Sadaoka, Y.; Traversa, E.; Sakamoto, M. *J. Mater. Chem.* **1996**, *6* (8), 1355. (c) Sakamoto, M.; Matsuki, K.; Ohsumi, R.; Nakayama, Y.; Matsumoto, A.; Okawa, H. *Bull. Chem. Soc. Jpn.* **1992**, *65*, 2278. (d) Sadaoka, Y.; Aono, H.; Traversa, E.; Sakamoto, M. *J. Alloys Compd.* **1998**, *278*, 135.

(2) (a) Imamura, H.; Miura, Y.; Fujita, K.; Sakata, Y.; Tsuchiya, S. *J. Mol. Catal. A* **1999**, *140*, 81. (b) Imamura, H.; Igawa, K.; Sakata, Y.; Tsuchiya, S. *Bull. Chem. Soc. Jpn.* **1996**, *69*, 325. (c) Imamura, H.; Igawa, K.; Kasuga, S.; Sakata, Y.; Tsuchiya, S. *J. Chem. Soc., Faraday Trans.* **1994**, *90*, 2119.

(3) (a) Rath, A.; Aceves, E.; Mitome, J.; Liu, J.; Ozkan, U. S.; Shore, S. G. *J. Mol. Catal. Commun.* **2001**, *165*, 103. (b) Shore, S. G.; Ding, E.; Park, C.; Keane, M. A. *Catal. Commun.* **2002**, *3*, 77. (c) Jujjuri, S.; Ding, E.; Shore, S. G.; Keane, M. A. *Appl. Organomet. Chem.* **2003**, *17*, 493.

10.1021/ic060756k CCC: $33.50
Published on Web 11/11/2006

Chart 1

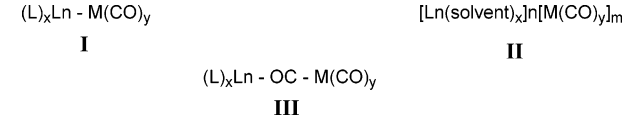

be arranged together in the presence of various ligands. New ways to synthesize compounds that hold metals of very different kinds in close proximity were developed.[5−10]

Extensive reviews on past research of Ln−M carbonyl complexes are available.[5] One can divide these complexes into three types (Chart 1):[5c] (**I**) systems with a direct Ln−M bond, (**II**) solvent-separated ion pairs, and (**III**) systems with isocarbonyl linkages.

Type **I** compounds are the most rare among the three, and to the best of our knowledge, only three X-ray structures have been reported.[6] Preparation techniques for these heterometallics include transmetalation,[5a,7] metathesis,[6b,8] M−M bond cleavage (reduction of the metal carbonyl dimers in liquid ammonia[6a,c,9] or over amalgam[10]), adduct formation,[8a,11] M−X bond cleavage,[8a,12] and condensation of solvent-separated ion pairs into extended arrays.[5a,b] The last approach appears to be especially valuable because it enables the preparation of polymeric structures with homogeneous distribution of the lanthanide and transition metal atoms. These materials are potentially important for preparing mixed Ln−M catalysts.[3,5] Such structures allow uniform dispersion of the metals over the support's surface.[2a]

Several such polymers containing Co linked to Yb or Eu were prepared recently in this laboratory.[5a,b] The starting material, in turn, was prepared via a transmetalation reaction between Ln metal and $Hg[Co(CO)_4]_2$ (reaction 1) . Solvent-

$$Yb + Hg[Co(CO)_4]_2 \xrightarrow[-Hg]{L} [Yb(L)_6][Co(CO_4)]_2 \qquad (1)$$

separated ion pair compounds of the general formula $[Yb(L)_n][Co(CO)_4]_2$ (L = THF, Pyr) were employed as starting materials, leading to two-dimensional arrays upon stirring with toluene (reaction 2). The present study continues this

$$[Yb(L)_n][Co(CO)_4]_2 \xrightarrow[-2Pyr\ \text{or}\ -2THF]{Tol} [(L)_xYb\{(\mu\text{-}CO)_yCo(CO)_{4-y}\}_2 \cdot zTol]_\infty \quad \begin{matrix} L = Pyr,\ x = 6y,\ y = 2,\ z = 0 \\ L = THF,\ x = 2,\ y = 3,\ z = 1 \end{matrix} \qquad (2)$$

research, shifting the emphasis from the transition metals of group VIII to those of group VII. Manganese-containing catalysts are widely used for the oxidative coupling and flameless combustion of methane,[13] and it would be of interest to prepare new types of potential catalyst precursors for such processes. Thus, the metals we worked with were Mn and Re.

Apart from the practical purpose of preparing new catalyst precursors, this work also investigates the influence of the solvent upon the products' structures. Competition[5b] between the solvent molecules and the transition metal carbonyl anion for the Ln^{n+} cation takes place in solution. If the metallic core of the anion possesses the greater electron-donating ability, then type **I** compounds form; on the other hand, if the solvent is the strongest electron donor available, then solvent-separated ion pairs (Type **II**) result. Finally, oxygen atoms of the carbonyl ligands can be electron donors through isocarbonyl bridges with a Type **III** complex being produced. Lewis basicity values are available for a wide range of organometallic species,[14] which should in principle help us to predict the reaction's outcome. But preliminary work shows that such an approach is not very reliable.

Results and Discussion

1. Transmetalation Reactions between Yb and $Hg[M(CO)_5]_2$ (M = Mn, Re). Direct reactions between Yb metal and $Hg[M(CO)_5]_2$ in various polar solvents produced solvent-separated ion-pair species $[Yb(L)_n][M(CO)_5]_2$ (M = Mn, **1**; Re, **2** reaction 3). With this approach, similar results

(4) (a) Baiker, A.; Marti, P. E.; Keusch, P.; Fritsch, E.; Reiller, A. *J. Catal.* **1994**, *146*, 268. (b) Lago, R.; Bini, G.; Pina, M. A.; Fierro, J. L. G. *World Congr. Oxid. Catal., Proc., 3rd; Stud. Surf. Sci. Catal.* **1997**, *110*, 721. (c) Yoshihko, S.; Enrico, T.; Sakamoto, M. *J. Alloys Compd.* **1996**, *240*, 51. (d) Buassi-Monroy, O. S.; Luhrs, C. C.; Chavez-Chavez, A.; Michel, C. R. *Mater. Lett.* **2004**, *58*, 716.
(5) (a) Plecnik, C. E.; Liu, S.; Liu, J.; Chen, X.; Meyers, E. A.; Shore, S. G. *Inorg. Chem.* **2002**, *41*, 4936. (b) Plecnik, C. E.; Liu, S.; Liu, J.; Chen, X.; Meyers, E. A.; Shore, S. G. *J. Am. Chem. Soc.* **2004**, *126*, 204. (c) Plecnik, C. E.; Liu, S.; Shore, S. G. *Acc. Chem. Res.* **2003**, *36*, 499.
(6) (a) Deng, H.; Shore, S. G.; *J. Am. Chem. Soc.* **1991**, *113*, 8538. (b) Beletskaya, I. P.; Voskoboynikov, A. Z.; Chuklanova, E. B.; Kirillova, N. I.; Shestakova, A. K.; Parshina, N. I.; Gusev, A. I.; Magomedov, G. K.-I. *J. Am. Chem. Soc.* **1993**, *115*, 3156. (c) Deng, H.; Chun, S.-H.; Florian, P.; Grandinetti, P. J.; Shore, S. G. *Inorg. Chem.* **1996**, *35*, 3891.
(7) (a) Lin, G.; Wong, W.-T. *Organomet. Chem.* **1996**, *522*, 271. (b) Suleimanov, G. Z.; Khandozhko, V. N.; Shifrina, R. R.; Abdullaeva, L. T.; Kolobova, N. E.; Beletskaya, I. P. *Dokl. Akad. Nauk SSSR* **1984**, *277*, 1407.
(8) (a) Crease, A. E.; Legzdins, P. *J. Chem. Soc., Dalton Trans.* **1973**, 1501. (b) Suleimanov, G. Z.; Beletskaya, I. P. *Dokl. Akad. Nauk SSSR* **1981**, *261*, 381. (c) Magomedov, G. K.-I.; Voskoboynikov, A. Z.; Chuklanova, E. B.; Gusev, A. I.; Beletskaya, I. P. *Metalloorg. Khim.* **1990**, *3*, 706.
(9) Voskoboynikov, A. Z.; Beletskaya, I. P. *Russ. Chem. Bull.* **1997**, *46*, 1789.
(10) (a) Beletskaya, I. P.; Suleimanov, G. Z.; Shifrina, R. R.; Mekhdiev, R. Y.; Agdamskii, T. A.; Khandozhko, V. N.; Kolobova, N. E. J. *Organomet. Chem.* **1986**, *299*, 239. (b) White, J. P., III; Deng, H.; Boyd, E. P.; Gallucci, J.; Shore, S. G. *Inorg. Chem.* **1994**, *33*, 1685.
(11) (a) Marks, T. J.; Kristoff, J. S.; Alich, A.; Shriver, D. F. *J. Organomet. Chem.* **1971**, *33*, C35. (b) Crease, A. E.; Legzdins, P. J. *J. Chem. Soc., Chem. Commun.* **1972**, *268*.
(12) Suleimanov, G. Z.; Khandozhko, V. N.; Mekhdiev R. Y.; Petrovskii, P. V.; Yanovskaya, I. M.; Lependina, O. L.; Kolobova, N. E.; Beletskaya, I. P. *Izv. Akad. Nauk SSSR, Ser. Khim.* **1988**, 685.
(13) (a) Pak, S.; Qui, P.; Lunsford, J. H. *J. Catal.* **1998**, *179*, 222. (b) Machocki, A.; Ioannides, T.; Stasinska, B.; Gac, W.; Avgouropoulos, G.; Delimaris, D.; Grzegorczyk, W.; Paseczna, S. *J. Catal.* **2004**, *227*, 282. (c) Tsyrulnikov, P. G.; Kovalenko, O. N.; Gogin, L. L.; Starostina, T. G.; Noskov, A. S.; Kalinkin, A. V.; Krukova, G. N.; Tsybulina, S. V.; Kudrina, E. N.; Bubnov, A. V. *Appl. Catal. A* **1998**, *167*, 31.
(14) (a) Dessey, R. E.; Pohl, R. L.; King, R. B. *J. Am. Chem. Soc.* **1966**, *88*, 5121. (b) King, R. B. *Acc. Chem. Res.* **1970**, *3*, 417.

$$Hg[M(CO)_5]_2 + Yb \xrightarrow{L} [Yb(L)_n][M(CO)_5]_2 + Hg \quad (3)$$

1, M = Mn, L = THF, $n = 6$

2, M = Re, L = THF, $n = 6$

1a, M = Mn, L = DME, *n* not established, presumably 4[15]

1b, M = Mn, L = DMF, *n* not established[15]

1c, M = Mn, L = pyridine, *n* not established, presumably 6[15]

were obtained for trivalent lanthanides with a number of transition metal anions,[5,7] and for divalent lanthanides with $[Co(CO)_4]^-$.[5] Despite a vast difference in Lewis basicity ($[Mn(CO)_5]^-$, 77; $[Re(CO)_5]^-$, 2.5×10^4; compared to the nucleophilicity of $[Co(CO)_4]^-$, which is set arbitrarily as 1)[14] and the softer Lewis acidic nature of Yb^{2+} compared to Yb^{3+}, the products are still ion-paired compounds with no isocarbonyl linkages formed. Anions $[M(CO)_5]^-$ (M = Mn, Re), were unable to penetrate the coordination sphere of solvent around the Yb^{2+} cation to replace THF molecules in their role as Lewis base. It has been shown[16] that the Lewis basicities of $[Co(CO)_4]^-$ and THF are similar (i.e., the basicity of THF should only slightly exceed 1). According to the results of Dessy et al.[14], it is inferior to values for anions studied herein. Our results suggest that an approach in which the electrophilic center (Yb^{2+} in this case) binds to the strongest Lewis base available[5,16] is not sufficient to predict what ligands will coordinate to the Yb^{2+} cation first.

Compounds with similar structure were synthesized by reduction of metal carbonyl dimers with lanthanide amalgam.[10] Using the methods described herein, we carried out the reduction of $Mn_2(CO)_{10}$ (but not that of $Re_2(CO)_{10}$) with ytterbium amalgam in THF and found that the product from this reaction is identical to **1** $[Yb(THF)_6][Mn(CO)_5]_2$ (reaction 4). Having established that, we routinely employed this

$$Yb/Hg + Mn_2(CO)_{10} \xrightarrow{THF} [Yb(THF)_6][Mn(CO)_5]_2 \quad (4)$$

procedure to synthesize **1**.

Syntheses analogous to reaction 3 were also carried out in diethyl ether and toluene. Earlier, a similar approach using $Hg[Co(CO)_4]_2$ yielded the previously unknown cluster[5b] $[Co_4(CO)_{11}]^{2-}$. In the present study, in both solvents, some reaction occurred as shown by a solution color change, and precipitation of a homogeneous mixture of product and a finely divided black powder. Unfortunately, the precipitates were only sparingly soluble, precluding the possibility of separating the products from the black material. Metallic mercury also precipitated along with the products, to produce a homogeneous mixture. For these reasons, no solid-state IR or elemental analyses were attempted. Upon removal of the original solvent and dissolution of the precipitates in THF, the IR spectra were like those of **1** and **2**, $[Yb(THF)_6][M(CO)_5]_2$. It is reasonable to assume some polymeric structures were formed in toluene and ether and cleaved later when THF was added to them.

Table 1. Infrared Data in the Carbonyl Stretching Frequency Region

compound	medium	ν_{CO} (cm^{-1})
$Mn_2(CO)_{10}$	THF or Et_2O	2045 (m, sh), 2008 (s, sh), 1980 (m, sh)
$Re_2(CO)_{10}$	THF or Et_2O	2070 (m, sh), 2009 (s, sh), 1966 (m, sh)
$KMn(CO)_5$	THF	2012 (vw), 1899 (s), 1865 (s), 1835 (m), 1896 (s), 1862 (s), 1830 (m)[a]
	Pyr	1978 (vw), 1897 (s), 1861(s)
$NaRe(CO)_5$	THF	2010 (vw), 1968 (w), 1910 (s) 1863 (s), 1830 (m), 1911 (s), 1864 (s), 1835 (sh)[a]
	Pyr	2009 (w), 1968 (mw), 1913 (s), 1860 (vs)
$Hg[Mn(CO)_5]_2$	KBr	2065 (s), 1995 (s, sh), 1955 (vs), 645(m),[b] 2067 (s), 2008 (sh),1975 (vs)[c]
$Hg[Re(CO)_5]_2$	Nujol	2073 (ms), 2014 (w, sh), 1974 (vs), 1935 (m, sh)[d]
	CH_2Cl_2	2075 (ms), 2024 (ms), 1995 (vs)[d]
1	THF	2011 (m to s), [1918 (s), 1892 (s), 1865 (m)], 1760 (ms)
2	THF	2043 (w), 2011 (s), 1972 (m), 1935 (s), 1890 (m), 1754 (m)
1a	DME	2012 (m), [1897 (s), 1864 (s)]
1b	DMF	2014 (vw), [1898 (s), 1865 (s)]
1c	Pyr	1978 (vw), [1897 (s), 1861 (s)]
	Et_2O	2015 (m), [1929 (s), 1903 (s)], 1724 (ms)
3	Et_2O	2015 (s, sh), 1931 (mw), 1908 (mw), 1707 (mw)

[a] Ellis, J. E.; Flom, E. A. *J. Organomet. Chem.* **1975**, *99*, 263. [b] Burlitch, J. M. *Chem. Commun.* **1968**, 887. [c] Hieber, W.; Schropp, W., Jr. *Chem. Ber.* **1960**, *93*, 455. [d] Hsieh, A. T. T.; Mays, M. J. *J. Chem. Soc. (A)* **1971**, 2648.

Solution IR Spectra of $[Yb(THF)_6][Mn(CO)_5]_2$ (1), $[Yb(THF)_6][Re(CO)_5]_2$ (2), $[Yb(DME)_n][Mn(CO)_5]_2$ (1a), $[Yb(DMF)_n][Mn(CO)_5]_2$ (1b), and $[Yb(pyr)_6][Mn(CO)_5]_2$ (1c). The IR spectra of compounds **1** and **1a** (Table 1) reveal features typical for solvent-separated ion-pair species. A thorough discussion of how such characteristic patterns arise can be found in the literature.[5a,16] In each spectrum, three groups of peaks can be clearly seen. The central group (in square parentheses in Table 1) strongly resembles the spectrum of the corresponding pure[17] $[M(CO)_5]^-$ anion in pyridine. These absorbances are assigned to the isolated transition metal carbonylate anion as it exists in solution of ligand. For **1**, this group is shifted to higher frequencies by about 5 cm^{-1} compared to the "pure" anion, suggesting that

(15) For **1a** and **1c**, the assignment of values of *n* was done by analogy with known complexes where cations $[Yb(DME)_4]^{2+}$ and $[Yb(pyr)_6]^{2+}$ are present.[5a] Elemental analysis was performed for **1c** indicating the presence of four pyridine molecules in the structure, but most probably some of the coordinated ligands were lost during sample preparation. In the case of **1b**, no data suggesting the number of DMF ligands coordinated around the Yb^{2+} center is available, but solution IR data clearly suggest that this is a solvent-separated ion-pair compound.

(16) (a) Edgell, W. F.; Yang, M. T.; Koizumi, N. *J. Am. Chem. Soc.* **1965**, *87*, 2563. (b) Edgell, W. F.; Lyford, J. IV; Barbetta, A.; Jose, C. I. *J. Am. Chem. Soc.* **1971**, *93*, 6403; Edgell, W. F.; Lyford, J. IV *J. Am. Chem. Soc.* **1971**, *93*, 6407. (c) Darensbourg, M. Y. *Prog. Inorg. Chem.* **1985**, *33*, 221.

(17) By the solution IR spectrum of the pure metal pentacarbonyl anion, we mean the spectrum which was recorded in strongly coordinating solvent, such as pyridine or DMF. Those solvents bind tightly to the cation and preclude any interaction between it and the carbonyl ligands of the anion, so that the latter's geometry is unaffected. Compare the spectra of **1**, **1c**, and $KMn(CO)_5$ in pyridine, Table 1.

some extra electron density is drained from the anion, probably through weak $(S)_nYb\cdots OCM(CO)_4$ interaction.[5a,18] For **1a**, the position of this group coincides with the $[Mn(CO)_5]^-$ spectrum, but an extra band appears on the left, which is discussed later. The spectra of **1b** and **1c** coincide entirely with the pure anion spectrum, with no extra peaks emerging. This is attributed to the very high Lewis basicities of pyridine and DMF, which enables them to bind to the Yb^{2+} cation strongly. Another two groups of peaks appear on the right and left sides of the central group. Their appearance can be accounted for in terms of formation of contact ion pairs.[5a,16] The IR spectrum of **2** is more complicated than that of **1**, but it can be analyzed along the same lines.

The difference in the spectra of **1c** in pyridine and in Et_2O is of interest. The compound was synthesized in pyridine, and its spectrum coincides completely with that of $Na[Mn(CO)_5]$ in the same solvent. However, when pyridine is removed and Et_2O added, the IR spectrum is very much like the spectra of **1**, **1a**, and **2**, with three distinct groups of peaks, indicating that contact ion pairs are present in solution. Both the pyridine solution and the Et_2O solution are dark brown, from which we conclude that even in ether solution some pyridine molecules are retained around the Yb^{2+} cation, but because some exchange occurs, the solvation layer is no longer impermeable, and an interaction between the ion pairs takes place.

X-ray Structures of 1 and 2. X-ray data were collected at −73 °C. Structures of the anions of these salts are represented in Figures 1 and 2. Because the $[Yb(THF)_6]^{2+}$ cation is essentially the same for both complexes, its structure is shown only once (Figure 1a). Crystallographic data and selected bond distances and angles are given in Tables 2 and 3. The $[Yb(THF)_6]^{2+}$ cation closely resembles its counterpart in the tetracarbonylcobaltate salt.[5] In both structures, two independent ytterbium atoms reside on inversion centers, each with three independent THF ligands; additional THF ligands are generated by symmetry transformations, resulting in nearly octahedral coordination of the Yb(II) centers. In **1**, the average Yb−O bond lengths are 2.392(4) and 2.391(6) Å; in **2**, these are 2.389(7) and 2.392(8) Å. In both structures, there is disorder indicated in the carbon atoms of the THF ligands. This cation, as reported elsewhere,[5] has Yb−O distances of 2.282(2), 2.387(2), and 2.396(3) Å. A shorter distance (2.298 Å) was reported for $[Yb(THF)_6][(nido\text{-}7,8\text{-}C_2B_9H_{11})_2]$.[19] Other Yb(II) compounds with coordinated THF ligands and their Yb−O bond lengths[5] include $[(MeOCH_2CH_2C_5H_4)_2Yb(THF)]$ (2.496(4) Å),[20a] $Cp^*_2Yb(THF)$ (2.412(5) Å),[20b] $(MeC_5H_4)_2Yb(THF)$ (2.53(2) Å),[20c] and $[\{Yb(Tp^{tBu,Me})(THF)(\mu\text{-}CO)_2Mo(\eta^5\text{-}C_5H_4Me)(CO)_3\}_2]$ (2.510(3) Å).[20d] For comparison, the Yb−O distances in $[Yb(DIME)_3][Co(CO)_4]_2$ (Yb 9-coordinated, tricapped trigonal arrangement) are from 2.49(1) to 2.69(2) Å.[10b]

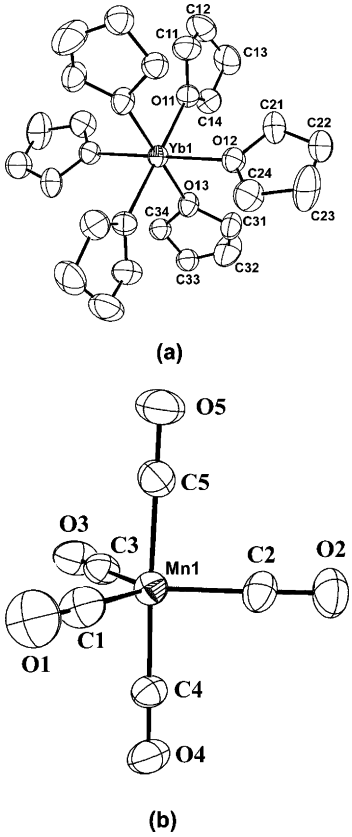

Figure 1. Molecular structure of **1**: (a) the $[Yb(THF)_6]^{2+}$ cation (25% thermal ellipsoids) and (b) the $[Mn(CO)_5]^-$ anion (15% thermal ellipsoids).

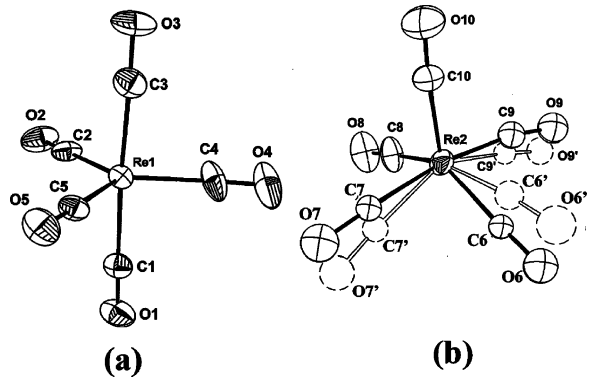

Figure 2. $[Re(CO)_5]^-$ anions in **2** (25% thermal ellipsoids): (a) anion without disorder and (b) disordered anion.

The manganese pentacarbonyl anion of **1** is similar to the same anion in other salts.[21] The structure contains two crystallographically independent anions, one of which is ordered and one disordered (see Supporting Information). In ordered $Mn(CO)_5$, the average Mn−C bond length is 1.795(9) Å, and the average C−O bond length is 1.155(8) Å.

We could find no record in the Cambridge X-ray Structure Database describing the $[Re(CO)_5]^-$ anion. It is reasonable

(18) Boncella, J. M.; Andersen, R. A. *Inorg. Chem.* **1984**, *23*, 432.
(19) Manning, M. J.; Knobler, C. B.; Khatter, R.; Hawthorne, M. F. *Inorg. Chem.* **1991**, *30*, 2009.
(20) (a) Deng, D.; Qian, C.; Song, F.; Wang, Z.; Wu, G.; Zheng, P. *J. Organomet. Chem.* **1993**, *443*, 79. (b) Tilley, T. D.; Andersen, R. A.; Spencer, B.; Ruben, H.; Zalkin, A.; Templeton, D. H. *Inorg. Chem.* **1980**, *19*, 2999. (c) Zinnen, H. A.; Pluth, J. J.; Evans, W. J. *J. Chem. Soc., Chem. Commun.* **1980**, 810. (d) Hillier, A. C.; Sella, A.; Elsegood, M. R. *J. Chem. Soc., Dalton Trans.* **1998**, 3871.
(21) (a) Frenz, B. A.; Ibers, J. A. *Inorg. Chem.* **1972**, *11*, 1109. (b) Corraine, M. S.; Lai, C. K.; Zhen, Y.; Churchill, M. R.; Buttrey, L. A.; Ziller, J. W.; Atwood, J. D. *Organometallics* **1992**, *11*, 35. (c) Kong, G.; Harakas, G. N.; Whittlesey, B. R. *J. Am. Chem. Soc.* **1995**, *117*, 3502.

Table 2. Crystallographic Data for $[Yb(THF)_6][M(CO)_5]_2$ (**1**, M = Mn; **2**, M = Re), $\{Yb(THF)_2(Et_2O)_2(Mn(CO)_5)_2\}_\infty$ (**3**), and $\{Yb(THF)_4(Mn(CO)_5)_2\}_\infty$ (**4**)

	1	**2**	**3**	**4**
empirical formula	$C_{34}H_{48}O_{16}Mn_2Yb$	$C_{34}H_{48}O_{16}Re_2Yb$	$C_{26}H_{36}O_{14}Mn_2Yb$	$C_{26}H_{32}Mn_2O_{14}Yb$
fw	995.64	1258.16	855.47	851.44
space group	$P\bar{1}$	$P\bar{1}$	$C2/c$	$C2/c$
a (Å)	10.8799(10)	10.0421(10)	16.7913(10)	11.3065(10)
b (Å)	11.1321(10)	10.7667(10)	10.3795(10)	18.9475(10)
c (Å)	19.5728(10)	19.7414(10)	19.6009(10)	15.6224(10)
α (deg)	78.261(10)	94.585(10)	90	90
β (deg)	89.715(10)	92.613(10)	93.357(10)	95.881(10)
γ (deg)	68.699(10)	92.898(10)	90	90
V (Å^3)	2156.3(3)	2122.3(3)	3410.2(4)	3329.2(4)
Z	2	2	4	4
D_{calcd} (g cm^{-3})	1.533	1.969	1.666	1.699
T (°C)	−73	−73	−73	−73
μ (mm^{-1})	2.790	7.939	3.509	3.594
$R_1[I > 2\sigma(I)]$[a]	0.0375	0.0517	0.0443	0.0362
R_2 (all data)[b]	0.1053	0.1400	0.1052	0.0870
GOF on F^2	1.029	1.076	1.020	1.058

[a] $R_1 = \sum||F_0| - |F_c||/\sum|F_0|$. [b] $R_2 = \{\sum w(F_0^2 - F_c^2)^2/\sum w(F_0^2)^2\}^{1/2}$.

Table 3. Selected Bond Distances (Å) and Angles (deg) for $[Yb(THF)_6][M(CO)_5]_2$ (**1**, M = Mn; **2**, M = Re)[a]

1		**2**	
Yb(1)−O(11)	2.400(4)	Yb(1)−O(11)	2.392(7)
Yb(1)−O(12)	2.385(4)	Yb(1)−O(12)	2.390(7)
Yb(1)−O(13)	2.392(4)	Yb(1)−O(13)	2.384(7)
Yb(2)−O(14)	2.388(4)	Yb(2)−O(14)	2.405(8)
Yb(2)−O(15)	2.390(4)	Yb(2)−O(15)	2.383(7)
Yb(2)−O(16)	2.394(4)	Yb(2)−O(16)	2.388(6)
M(1)−C(1)	1.829(8)	M(1)−C(1)	1.971(13)
M(1)−C(2)	1.775(9)	M(1)−C(2)	1.932(14)
M(1)−C(3)	1.797(8)	M(1)−C(3)	1.966(14)
M(1)−C(4)	1.778(8)	M(1)−C(4)	1.935(12)
M(1)−C(5)	1.796(9)	M(1)−C(5)	1.941(12)
C(2)−O(2)	1.160(9)	C(2)−O(2)	1.154(14)
C(4)−O(4)	1.163(8)	C(4)−O(4)	1.175(15)
C(1)−O(1)	1.143(8)	C(1)−O(1)	1.141(14)
C(3)−O(3)	1.153(8)	C(3)−O(3)	1.157(15)
C(5)−O(5)	1.154(8)	C(5)−O(5)	1.138(13)
O(12)−Yb(1)−O(13)	89.46(13)	O(12)−Yb(1)−O(13)	88.3(3)
O(11)−Yb(1)−O(12)	89.76(15)	O(11)−Yb(1)−O(12)	89.8(3)
O(11)−Yb(1)−O(13)	89.29(14)	O(11)−Yb(1)−O(13)	89.7(3)
C(1)−M(1)−C(3)	178.5(3)	C(1)−M(1)−C(3)	175.6(6)
C(2)−M(1)−C(4)	116.9(4)	C(2)−M(1)−C(4)	118.1(7)
C(2)−M(1)−C(5)	121.2(4)	C(2)−M(1)−C(5)	116.8(5)
C(4)−M(1)−C(5)	121.9(4)	C(4)−M(1)−C(5)	124.9(6)
C(3)−M(1)−C(2)	90.0(4)	C(3)−M(1)−C(2)	94.7(5)
C(3)−M(1)−C(4)	90.5(3)	C(3)−M(1)−C(4)	92.1(6)
C(3)−M(1)−C(5)	89.8(3)	C(3)−M(1)−C(5)	88.1(5)

[a] Data for the nondisordered $[M(CO)_5]^-$ anions are given.

to assume that this anion would be analogous to $[Mn(CO)_5]^-$. In the structure of **2**, there are also two $[Re(CO)_5]^-$ anions, one of them possessing trigonal bipyramidal geometry, analogous to that of $[Mn(CO)_5]^-$ (Figure 2a), and the other distorted and disordered (see Supporting Information). The average Re−C distance is 1.949(14) Å, and that of C−O is 1.153(15) Å. All angles are close to the values for a trigonal bipyramid, and the axial bond distances appear to be longer than the equatorial ones (Table 3).

Normally, transition metal pentacarbonyls possess trigonal bipyramidal coordination, as observed for isoelectronic $[M(CO)_5]^{2-}$ (M = Cr, Mo, W),[22] $[Mn(CO)_5]^-$, and $Fe(CO)_5$.[23] Angles between base ligands vary from 81.0(10) to 89.1(10)°, and those between axial and base ligands vary from 95.3(12) to 113.7(11)°. To the best of our knowledge, there is only one previously known example of a pentacarbonyl transition metal anion with square pyramidal geometry,[24] the $[Mn(CO)_5]^-$ anion in the complex $[Ph_4P][Mn(CO)_5]$.

Condensation of 1 with Et_2O into Extended Structures $\{Yb(THF)_2(Et_2O)_2[(\mu\text{-}CO)_2Mn(CO)_3]_2\}_\infty$ (3) and $\{Yb(THF)_4[(\mu\text{-}CO)_2Mn(CO)_3]_2\}_\infty$ (4). It has been shown that dissolution of $[Ln(S)_6][Co(CO)_4]_2$ (S = THF, pyridine) in diethyl ether and toluene facilitates condensation of solvent-separated ion pairs into extended linear structures or two-dimensional arrays where the cation and the anion are linked together by isocarbonyl bridges.[5] In diethyl ether, novel cobalt clusters that are still bonded to the lanthanide moiety through bridging isocarbonyls were obtained.[5b] We carried out similar reactions on salts **1** and **2**. Condensation with ether, but not with toluene, proved to be possible for **1** (reaction 5),

$$\underset{\mathbf{1}}{[Yb(THF)_6][Mn(CO)_5]_2} \xrightarrow[\text{1-2 days}]{Et_2O} \underset{\mathbf{3}}{\{(THF)_2(Et_2O)_2Yb[(\mu\text{-}CO)_2Mn(CO)_3]_2\}_\infty} \quad (5)$$

which is poorly soluble in Et_2O; however, after the mixture was stirred overnight, a green solution was obtained, and a vast quantity of undissolved material remained in the reaction flask. Emerald-green crystals grown from this solution, compound **3**, have a sheet structure, as elucidated by single-crystal X-ray analysis (Figures 3 and 4). These crystals had to be grown relatively rapidly, taking no more than 2 days to evaporate the solvent. When the original solution was allowed to spend some time in the flask, or evaporated more slowly (7−10 days), some black decomposition products precipitated, and the solution gradually changed from green

(22) (a) Kaska, W. C. *J. Am. Chem. Soc.* **1968**, *90*, 6340. (b) Anastassiou, A. G.; Elliot, R. L.; Reichmanis, E. *J. Am. Chem. Soc.* **1974**, *96*, 7825. (c) Darensbourg, M. Y.; Slater, S. *J. Am. Chem. Soc.* **1981**, *103*, 5914. (d) Maher, J. M.; Beatty, R. P.; Cooper, N. J. *Organometallics* **1985**, *4*, 1354.

(23) (a) Hanson, A. W. *Acta Crystallogr.* **1962**, *15*, 930. (b) Donohue, J.; Caron, A. *Acta Crystallogr.* **1964**, *17*, 663.

(24) Seidel, R.; Schautz, B.; Henkel, G. *Angew. Chem., Int. Ed. Engl.* **1996**, *35*, 1710.

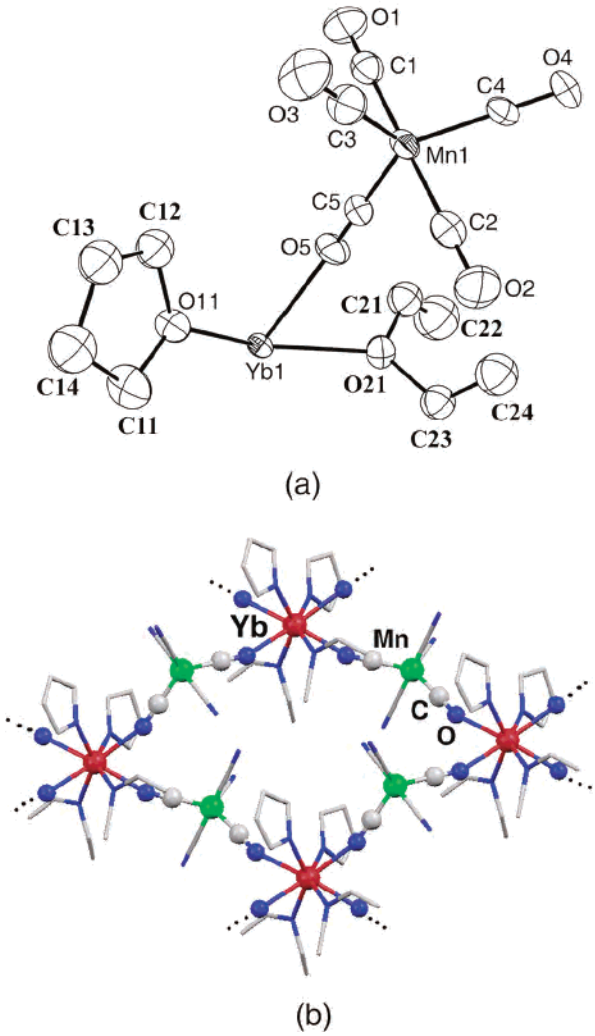

Figure 3. Molecular structure of **3**: (a) asymmetric unit (25% thermal ellipsoids) and (b) eight-member ring.

to yellow and yellow crystals of **4**, $\{Yb(THF)_4[(\mu\text{-}CO)_2Mn(CO)_3]_2\}_\infty$, appeared (reaction 6). The latter compound is a

$$\underset{\mathbf{1}}{[Yb(THF)_6][Mn(CO)_5]_2} \xrightarrow[7-10\ \text{days}]{Et_2O} \underset{\mathbf{4}}{\{(THF)_4Yb[(\mu\text{-}CO)_2Mn(CO)_3]_2\}_\infty} \quad (6)$$

chain (Figure 5).

A freshly prepared solution of **1** in Et_2O, upon standing at room temperature, is noticeably converted to **3**, the IR spectrum of which consists of one strong sharp absorption in the terminal carbonyl region, 2015 cm^{-1}, and three medium to weak bands at 1931, 1908, and 1707 cm^{-1}. In 24 h, the peak at 2015 cm^{-1} remains almost as strong, while the intensity of the others diminishes significantly. After more time (4−6 days), two new peaks begin to emerge at 2046 and 1978 cm^{-1}. This new spectrum corresponds to the spectrum of $Mn_2(CO)_{10}$, with crystals of **4** growing simultaneously with formation of the $Mn_2(CO)_{10}$, and a black powder.

The following pathways for formation of **3** and **4** are proposed. It is reasonable to assume that when complex **1** is

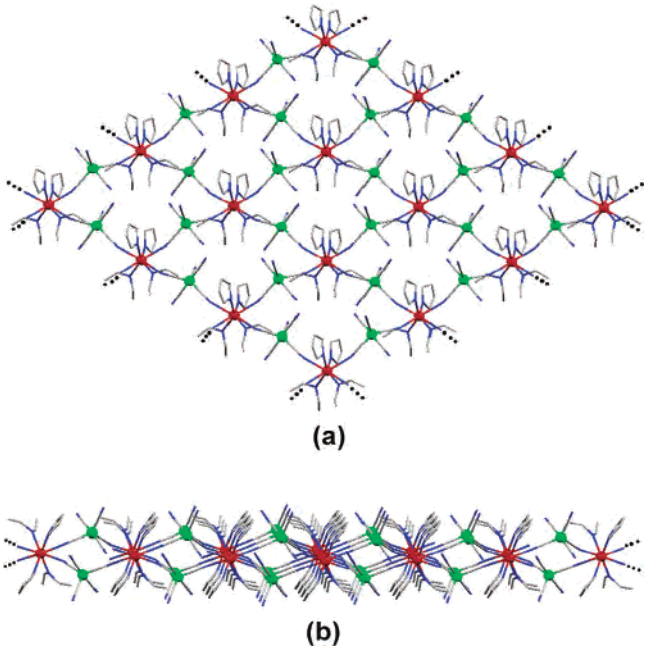

Figure 4. Views of a portion of the 2-D polymeric sheet of **3**: (a) top view (along the *c* axis) and (b) cross-section (view along *b* axis). Ytterbium atoms shown in red, manganese in green, carbon in gray, and oxygen in blue.

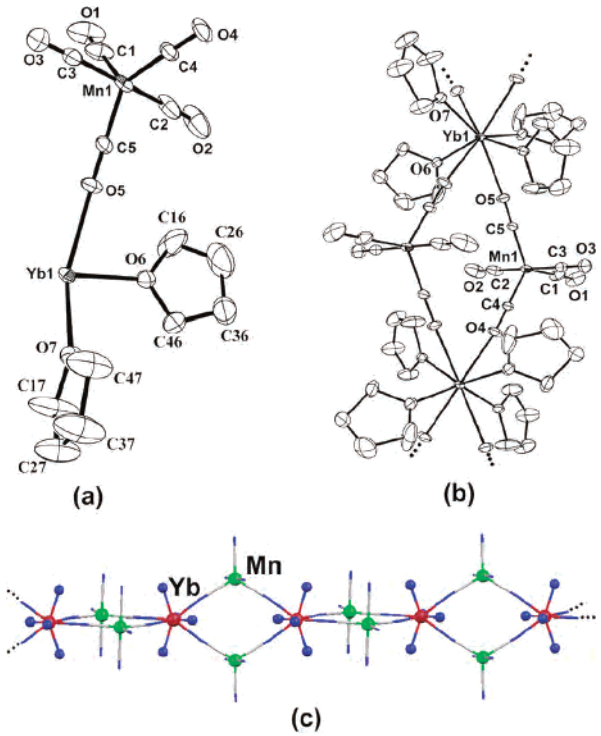

Figure 5. Molecular structure of **4**: (a) asymmetric unit (25% thermal ellipsoids), (b) a diamond (15% thermal ellipsoids), and (c) portion of a 1-D linear chain of **4** (only oxygen atoms of THF ligands are shown for clarity)

added to Et_2O, some THF ligands dissociate from the Yb^{2+} core, leaving coordination sites vacant for other Lewis bases. Those vacant sites are then filled with oxygen atoms of $[Mn(CO)_5]^-$ and Et_2O, thus forming diamond-shaped clusters that combine to form crystals of **3** (Figures 3−4). The clusters contain both THF and Et_2O as ligands coordinated to the cation. However, complex **3** is unstable in Et_2O. It slowly

converts to complex **4** (Figure 5), a reaction in which $[Mn(CO)_5]^-$ is oxidized to form $Mn_2(CO)_{10}$. In addition to the oxidation of $[Mn(CO)_5]^-$, it is believed that Yb^{2+} is reduced to Yb^0, which precipitates as the black powder described previously. Earlier, we observed that the solvent-separated ion pairs[5b] $[Ln(THF)_6][Co(CO)_4]$ (Ln = Yb, Eu, $x = 6$), when placed in Et_2O, undergo reactions in which $[Co(CO)_4]^-$ is oxidized to form the previously unreported cluster $[Co_4(CO)_{11}]^-$ that is linked to the lanthanide through isocarbonyl linkages. As in the present case, a black powder is also produced that is attributed to the formation of the reduced lanthanide. Unfortunately, this finely divided powder is dispersed thoughout the polymeric sample and, as in the present case, could not be separated from it for positive identification of Ln^0.

A reviewer of this manuscript does not accept this interpretation arguing that $Mn(CO)_5^-$ is insufficiently reducing to form Ln(0) in its conversion to $Mn_2(CO)_{10}$; however, we respectfully disagree. We are reluctant to assign the black powder observed in this and in the reactions of $[Co(CO)_4]^-$ with lanthanides[5] to degradation processes and side reactions.

Another possibility that has been suggested for the formation of $Mn_2(CO)_{10}$ and the black powder from $[Mn(CO)_5]^-$ is the disproportionation of $[Mn(CO)_5]^-$ to $Mn_2(CO)_{10}$ and Mn. However, we believe this possiblity to be remote. We are unaware of $[Mn(CO)_5]^-$ normally undergoing spontaneous disproportionation to give Mn and $Mn_2(CO)_{10}$. If the $[Mn(CO)_5]^-$ disproportionates when the THF is replaced by Et_2O, then Yb^{2+} is an "innocent bystander", and another anion is required to compensate for the excess Yb^{2+} when $[Mn(CO)_5]^-$ is oxidized and condensed to $Mn_2(CO)_{10}$. Furthermore, since manganese is in the minus one oxidation state in $[Mn(CO)_5]^-$, the formation of metallic Mn from $[Mn(CO)_5]^-$ involves oxidation rather than reduction, and then the question remains, what has been reduced? We believe it to be Yb^{2+}. It is well-known in coordination chemistry that the stability of the oxidation state of a metal can depend on the base strengths of the associated ligands. The weaker basicity of Et_2O compared to THF would present a weaker barrier for electron transfer to Yb^{2+} than THF. Diethyl ether is a significantly weaker base than THF. For example, Et_2O does not cleave the bridge system of B_2H_6, while THF readily reacts with B_2H_6 to form $THF{\cdot}BH_3$.

The redox reaction 7 can be written as decomposition of

$$Yb^{2+} + 2[Mn(CO)_5]^- \xrightarrow{Et_2O} Yb^0 + Mn_2(CO)_{10} \qquad (7)$$

3 to **4** (reaction 8). The fact that it takes more time to form

$$2\{(THF)_2(Et_2O)_2Yb[(\mu\text{-}CO)_2Mn(CO)_3]_2\}_\infty \xrightarrow{Et_2O} \underset{\mathbf{3}}{} \{(THF)_4Yb[(\mu\text{-}CO)_2Mn(CO)_3]_2\}_\infty + \underset{\mathbf{4}}{} Yb + 1/2\ Mn_2(CO)_{10} + 4Et_2O \qquad (8)$$

crystals of **4** suggests that it is a thermodynamic product, while the structure of **3** is a kinetic one.

Table 4. Selected Bond Lengths (Å) and Angles (deg) for $\{Yb(THF)_2(Et_2O)_2[(\mu\text{-}(CO)_2Mn(CO)_3)_2]\}_\infty$ (**3**) and $\{Yb(THF)_4[(\mu\text{-}(CO)_2Mn(CO)_3)_2]\}_\infty$ (**4**)

3		**4**	
Mn(1)−C(1)	1.836(9)	Mn(1)−C(1)	1.823(6)
Mn(1)−C(2)	1.834(9)	Mn(1)−C(2)	1.810(7)
Mn(1)−C(3)	1.800(9)	Mn(1)−C(3)	1.830(6)
Mn(1)−C(4)	1.759(8)	Mn(1)−C(4)	1.773(4)
Mn(1)−C(5)	1.777(8)	Mn(1)−C(5)	1.775(4)
C(1)−O(1)	1.117(8)	C(1)−O(1)	1.183(15)
C(2)−O(2)	1.136(9)	C(2)−O(2)	1.197(15)
C(3)−O(3)	1.164(9)	C(3)−O(3)	1.138(7)
C(4)−O(4)	1.179(8)	C(4)−O(4)	1.169(5)
C(5)−O(5)	1.165(8)	C(5)−O(5)	1.168(5)
Yb(1)−O(11)	2.470(4)	Yb(1)−O(6)	2.456(3)
Yb(1)−O(21)	2.473(5)	Yb(1)−O(7)	2.468(3)
Yb(1)−O(4)	2.502(5)	Yb(1)−O(4)	2.507(3)
Yb(1)−O(5)	2.486(5)	Yb(1)−O(5)	2.521(3)
C(2)−Mn(1)−C(1)	177.5(4)	C(2)−Mn(1)−C(3)	179.1(3)
C(5)−O(5)−Yb(1)	158.8(6)	C(5)−O(5)−Yb(1)	174.8(4)
C(4)−O(4)−Yb(1)	159.4(5)	C(4)−O(4)−Yb(1)	173.5(4)
O(11)−Yb(1)−O(11)	109.6(2)	O(6)−Yb(1)−O(6)	93.50(19)
O(21)−Yb(1)−O(21)	111.4(2)	O(7)−Yb(1)−O(7)	90.48(15)
O(4)−Yb(1)−O(4)	119.3(3)	O(4)−Yb(1)−O(4)	138.32(18)
O(11)−Yb(1)−O(4)	72.60(16)	O(6)−Yb(1)−O(4)	72.35(13)
O(21)−Yb(1)−O(5)	72.40(18)	O(7)−Yb(1)−O(4)	74.49(12)

The attempted analytical confirmation of the stoichiometry of reaction 8 encountered certain difficulties. First, **3** proved to be difficult to redissolve in Et_2O, no doubt because of its polymeric nature. Also, both **4** and the Yb metal precipitate required separation that led to loss of products and greater experimental errors. Despite this, determination of the amount of ytterbium produced in reaction 8 was found to correspond approximately to what is expected from the proposed process's stoichiometry.[27] That, along with the fact that solution IR of the mother liquor of **4** reveals the presence of $Mn_2(CO)_{10}$, confirming the oxidation of $[Mn(CO)_5]^-$.

Molecular Structure of 3. The structure is represented in Figures 3 and 4. Crystallographic data are given in Table 2; selected bond distances and angles are given in Table 4. In the structure of **3**, half of an Yb atom, two ligands (THF and Et_2O, Figure 3a), and one manganese pentacarbonylate anion form the asymmetric unit. Symmetry transformations of these unique atoms generate a nonplanar polymeric sheet (Figure 4a). The axial "poles" (constructed of the two axial carbonyls and the manganese atom) of the two manganese pentacarbonylate anions attached to the same ytterbium atom are almost exactly perpendicular to each other. In **3**, four

(25) http://www.webelements.com/webelements/elements/text/Yb/red.html

(26) (a) Dessy, R. E.; Weissman, P. M.; Pohl, R. L. *J. Am. Chem. Soc.* **1966**, *88*, 5117. (b) Corraine, M. S.; Atwood, J. D. *Organometallics* **1991**, *10*, 2315. (c) Pugh, J. R.; Meyer, T. J. *J. Am. Chem. Soc.* **1992**, *114*, 3784.

(27) Two hundred forty milligrams of **3** was dissolved in 50 mL of diethyl ether, and the solution was allowed to sit in the flask for 7 days. A black precipitate appeared, along with the crystals of **4**. The remaining solution was then removed, and the precipitate was washed with THF to separate ytterbium metal (compound **4** dissolves in THF, apparently producing **1**). Sixty-nine milligrams of the black material was collected. The analysis performed by Galbraith Laboratories, Inc., showed 42.42% ytterbium content, which amounts to 29.3 mg of ytterbium metal. On the basis of stoichiometry of reaction 8, 24.2 mg is expected. The explanation of this difference could possibly be that not all of the **4** was washed off, thus contributing to ytterbium content of the sample.

Table 5. Selected Bond Distances (Å) and Angles (deg) for $[(THF)_5Yb(\mu\text{-}CO)Mn_3(CO)_{13}][Mn_3(CO)_{14}]$ (**6**)

Yb(1)−O(5)	2.378(4)	C(14)−O(14)	1.143(5)
Yb(1)−O(6)	2.369(3)	C(15)−O(15)	1.148(6)
Yb(1)−O(7)	2.382(4)	C(21)−O(21)	1.151(8)
Yb(1)−O(8)	2.383(4)	C(22)−O(22)	1.145(8)
O(24)−Yb(1)	2.437(4)	C(23)−O(23)	1.137(7)
Mn(1)−Mn(2)	2.8841(7)	C(24)−O(24)	1.171(7)
Mn(3)−Mn(4)	2.9023(7)	Mn(3)−C(31)	1.829(5)
Mn(1)−C(11)	1.828(6)	Mn(3)−C(32)	1.828(5)
Mn(1)−C(12)	1.801(6)	Mn(4)−C(41)	1.837(5)
Mn(1)−C(13)	1.837(5)	Mn(4)−C(42)	1.842(5)
Mn(1)−C(14)	1.824(5)	Mn(4)−C(43)	1.839(5)
Mn(1)−C(15)	1.834(5)	Mn(4)−C(44)	1.842(5)
Mn(2)−C(21)	1.826(7)	Mn(4)−C(45)	1.810(5)
Mn(2)−C(22)	1.829(7)	C(31)−O(31)	1.148(5)
Mn(2)−C(23)	1.837(6)	C(32)−O(32)	1.147(5)
Mn(2)−C(24)	1.790(6)	C(41)−O(41)	1.144(6)
C(11)−O(11)	1.140(6)	C(42)−O(42)	1.141(6)
C(12)−O(12)	1.147(6)	C(43)−O(43)	1.144(6)
C(13)−O(13)	1.136(5)	C(44)−O(44)	1.141(5)
		C(45)−O(45)	1.140(5)

Mn(1)#1−Mn(2)−Mn(1)	172.62(4)	C(24)−Mn(2)−C(21)	179.5(3)
C(11)−Mn(1)−Mn(2)	88.3(2)	C(22)−Mn(2)−C(21)	88.2(3)
C(12)−Mn(1)−Mn(2)	174.22(16)	C(45)−Mn(4)−Mn(3)	178.00(15)
C(13)−Mn(1)−Mn(2)	83.25(15)	C(41)−Mn(4)−Mn(3)	83.43(16)
C(14)−Mn(1)−Mn(2)	78.58(15)	C(42)−Mn(4)−Mn(3)	83.52(15)
C(15)−Mn(1)−Mn(2)	87.43(17)	C(43)−Mn(4)−Mn(3)	85.76(16)
C(21)−Mn(2)−Mn(1)	86.35(2)	C(44)−Mn(4)−Mn(3)	82.11(14)
C(22)−Mn(2)−Mn(1)	90.42(2)	C(31)−Mn(3)−Mn(4)	90.60(14)
C(23)−Mn(2)−Mn(1)	89.50(2)	C(41)−Mn(4)−C(42)	166.9(2)
C(24)−Mn(2)−Mn(1)	93.66(2)	C(41)−Mn(4)−C(43)	90.4(2)
C(15)−Mn(1)−C(11)	89.4(2)	C(41)−Mn(4)−C(44)	90.7(2)
C(12)−Mn(1)−C(11)	94.4(3)	C(32)−Mn(3)−C(31)	89.6(2)

ytterbium and four manganese atoms bound by isocarbonyl linkages form rings (Figure 3b) containing 4 $Mn(CO)_5$ and $4Yb(THF)_2(Et_2O)_2$ units, similar to $\{(Pyr)_4Yb[(\mu\text{-}CO)_2Co(CO)_2]_2\}_\infty$[5]. A cross-section of this zigzag puckered sheet (Figure 4b) shows that the $Mn(CO)_5$ units lie above and below the plane containing the Yb atoms, as in the compound cited above. The C−O−Yb angles are 158.8(6) and 159.4(5)°, noticeably less than 180°, indicating internal constraints in the structure. Significant disorder was present in the carbon atoms of THF and in some oxygen atoms of CO. The Yb−O bond distances to THF, 2.470(4) and 2.473(5) Å, are longer than those in **1** and **2**, corresponding to the large (8-fold) coordination number of Yb here. The Mn−C distances in **3** are of two types, terminal (average 1.769(8) Å) and bridging (average 1.823(9) Å), with average C−O distances of 1.172(8) and 1.139(9) Å, respectively. Some disorder is observed in THF and Et_2O ligands in this structure (see Supporting Information).

Molecular Structure of 4. The molecular structure of **4** is shown in Figure 5. Crystallographic data are given in Table 2, and selected bond distances and bond angles are given in Table 4. As in compound **3**, the asymmetric unit of **4** consists of half of an Yb atom, two ligands, and one pentacarbonylmanganese anion. The substantial difference is that the two ligands coordinated to the Yb^{2+} center are both THF molecules (in **3**, one is a THF molecule and the other one is Et_2O). Symmetry transformations of the unique atoms generate a one-dimensional polymeric chain (Figure 5). Linear chains of **4** are composed of four-member diamonds (Figure 5b) that have alternatively two ytterbium and two manganese atoms at their vertexes, the former being the diamonds' connection points. Each diamond is planar, with its plane perpendicular to the planes of its two neighbors (Figure 5c). The four THF ligands are located around the Yb^{2+} cation according to the principle of least repulsion, thus lying on bisectors of dihedral angles formed by the plane of one diamond and the edge of another. The C−O−Yb angles (174.8(4) and 173.5(4)°) are closer to 180° than corresponding angles in **3**, suggesting the greater stability of structure **4**.

The Yb^{2+} center in both structures **3** and **4** is 8-coordinated and possesses a distorted square-antiprism geometry. The Yb1 atom lies on a 2-fold rotation axis. The vertexes of the square antiprism are occupied by oxygen atoms of alternating ligand molecules and $[Mn(CO)_5]^-$ anions. In **3**, the Yb−O(THF) and Yb−O(Et_2O) distances are 2.470(4) and 2.473(5) Å, respectively; in **4**, the Yb−O(THF) bond lengths are 2.456(3) and 2.468(3) Å. In both compounds, the Yb−O(THF) bonds are about the same length and are longer then those in **1** and **2**: this is believed to be caused by donation of some electron density from the manganese pentacarbonylate anion to ytterbium.[5,18] Each anion is bound to two Yb(II) centers through two of its equatorial carbonyls. The C−O distances of the bridging ligands (**3**, 1.179(8) and 1.165(8) Å; **4**, 1.169(5) and 1.168(5) Å) are greater than those of nonbridging equatorial carbonyls (**3**, 1.164(9) Å; **4**, 1.183(15) Å) and three of the four axial ligands (**3**, 1.118(8) and 1.136(9) Å; **4**, 1.197(15) and 1.138(7) Å). In both structures, the C−Mn−C angles deviate slightly from perfect trigonal bipyramidal geometry. Some disorder is observed carbonyl and THF ligands in this structure (see Supporting Information).

Minor Products of Condensation of 1 with Et_2O. Molecular Structures of $(THF)_2Mn_3(CO)_{10}$ (5) and $[(THF)_5Yb(\mu\text{-}CO)Mn_3(CO)_{13}][Mn_3(CO)_{14}]$ (6). After compound **4**, with some mother liquor, was allowed to sit in a flask for 3 weeks, ruby-red crystals of **5** formed in the mixture with the original crystals of **4**. This compound was synthesized and characterized previously[28] via the reaction of $Mn_2(CO)_{10}$ with $AlMe_3$ in a mixture of THF and hexanes, which led to several products, including **5**. The authors could not reproduce their synthesis: all repeated attempts to isolate compound **5** only led to formation of $Mn_2(CO)_{10}$. Unfortunately, we could not duplicate the synthesis either. Nevertheless, we report this result as confirmation of the existence of $(THF)_2Mn_3(CO)_{10}$ and proof of its relative stability. Repeated efforts to prepare **5** resulted either in no reaction or formation of $[(THF)_5Yb(\mu\text{-}CO)Mn_3(CO)_{13}][Mn_3(CO)_{14}]$, **6** (Figure 6).

The crystallographic data for compound **5**, selected bond distances and angles, and its molecular structure are given in the Supporting Information. Complex **5** is predicted to be paramagnetic,[29] and it would be interesting to prepare a sufficiently large quantity of this material to investigate its magnetic properties.

(28) Kong, G.; Harakas, G. N.; Whittlesey, B. R. *J. Am. Chem. Soc.* **1995**, *117*, 3502.
(29) Xu, Z., Lin, Z. *Chem.—Eur. J.* **1998**, *4*, 28.

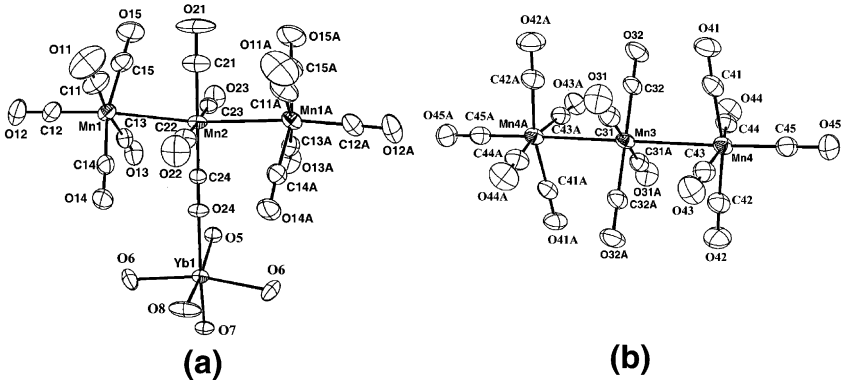

Figure 6. Molecular structure of **6** (35% probability ellipsoids shown): (a) the $[(THF)_5Yb(\mu\text{-}CO)Mn_3(CO)_{13}]^+$ cation (only oxygen atoms of THF shown) and (b) the $[Mn_3(CO)_{14}]^-$ anion.

Ion-paired compound **6** tends to form more predictably than **5**, crystallizing in about 3 to 4 weeks in the flask containing crystals of **4** with some mother liquor from which the latter was grown. This process is reproducible but every time with a different degree of success. We were unable to determine what conditions favor the formation of **6**. The analogous molecule $Mn_2Fe(CO)_{14}$ has been prepared by UV photolysis of an equimolar solution of $Fe(CO)_5$ and $Mn_2(CO)_{10}$ in *n*-hexane.[30] Dark-red crystals of **6** are always mixed with **4**, and both **4** and **6** are soluble and insoluble in the same sets of solvents. For these reasons, no elemental analysis or infrared data were obtained.

Crystallographic data for compound **6** and selected bond distances and bond angles are presented in the Supporting Information. Complex **6** is an ionic compound that contains a rarely observed anion, $[Mn_3(CO)_{14}]^-$, which is isoelectronic with $Mn_2Fe(CO)_{14}$[30] and has similar geometry. It was first reported by Curtis,[31] and its X-ray structure was published by Bau and collegues.[32] Uniquely, there are two such units in our structure and one of them is connected to the Yb^{II} center through an isocarbonyl linkage, thus forming the complex cation $[(THF)_5Yb(\mu\text{-}CO)Mn_3(CO)_{13}]^+$ (Figure 6a) (the other $[Mn_3(CO)_{14}]^-$ anion remains free). In this cation, ytterbium has distorted octahedral coordination. The isocarbonyl bridge belongs to the central manganese atom of the $[Mn_3(CO)_{14}]$ core, and four out of five THF ligands are disordered. In the free $[Mn_3(CO)_{14}]^-$ anion (Figure 6b), the central Mn atom resides on a center of inversion; thus there is one unique $Mn(CO)_5$ moiety and two carbonyl ligands attached to the central manganese, the rest of the anion being symmetry generated. While the free anion possesses crystallographically imposed linear character and is of D_{4h} symmetry, the anion bound to the Yb atom is slightly bent (Mn(1)−Mn(2)−Mn(1)′ angle = 172.62(4)°), and Mn(2) lies on a mirror plane. In the complex cation, the Mn−Mn distance (2.8841(7) Å) is shorter than that in $Mn_2(CO)_{10}$ (2.9042(8) Å);[33] the length of the same bond in the free anion (2.9023(7) Å) is closer to the value for the manganese carbonyl dimer. For the bridging carbonyl, the Mn−C distance (1.790(6) Å) is significantly shorter than corresponding distances for the equatorial CO ligands (1.830(7) Å average). For comparison, average Mn−C distances in $Mn_2Fe(CO)_{14}$ are 1.855(10) (equatorial) and 1.805(10) Å (axial). The reasons for such length differences were thoroughly discussed elsewhere.[32] In both free and bound $[Mn_3(CO)_{14}]$ units, equatorial carbonyls of $Mn(CO)_5$ groups are bent inward, a phenomenon that has been observed for a number of carbonyl-containing systems.[32] In the bound $[Mn_3(CO)_{14}]$ unit, this is slightly more pronounced for one of the ligands (C(14)−Mn(1)−Mn(2) = 78.58(15)°) than for any other (85(2)°, averaged over both bound and free anions). The Yb−O(OC) distance (2.437(4) Å) is longer then any of the Yb−O(THF) distances (2.378(4) Å).

In conclusion, a series of new lanthanide−transition metal compounds was prepared. Solvent-separated ion-paired species **1**, **1a**, **1b**, **1c**, and **2** were synthesized first, and compound **1** was then converted into polymeric structures **3** and **4**, containing isocarbonyl linkages. The conversion was achieved by stirring **1** with diethyl ether, which facilitated condensation of separated cations and anions into a polymer. Compound **3**, formed initially, has a layer sheet structure. Compound **4**, formed after an extended time from the mother liquor of **3**, is a one-dimensional chain. Minor products **5** and **6** were observed and characterized by single-crystal X-ray diffraction.

Experimental Section

General Procedures. All manipulations were carried out on a standard high-vacuum line or in a drybox under a nitrogen or argon atmosphere. Diethyl ether, tetrahydrofuran, pyridine, toluene, and 1,2-dimethoxyethane (DME) were dried over sodium/benzophenone and freshly distilled prior to use. *N*,*N*-Dimethylformamide (DMF) was shaken over type 4 Å Linde molecular sieves for 48 h. The sieves and Celite were dried under dynamic vacuum for 18 h at 130 °C prior to use. Ytterbium powder (Strem) and metallic mercury (Bethlehem Apparatus, Inc., quadruple-distilled) were used as received. Dimanganese decacarbonyl and dirhenium decacarbonyl (Aldrich) were purified by vacuum sublimation at 100 °C. Elemental analyses were performed by Galbraith Laboratories, Inc. (Knoxville, TN). Prolonged pumping on crystalline samples caused loss of solvent ligands. Therefore, samples of compounds **1** and **2** were sent to the analytical laboratory packed in dry ice, and analyses

(30) Agron, P. A.; Ellison, R. D.; Levy, H. A. *Acta Crystallogr.* **1967**, *23*, 1079.
(31) Curtis, M. D. *Inorg. Chem.* **1972**, *11*, 802.
(32) Bau, R.; Kirtley, S. W.; Sorrell, T. N.; Winarko, S. *J. Am. Chem. Soc.* **1974**, *96*, 988.
(33) Bianchi, R.; Gervasio, G.; Marabello, D. *Inorg. Chem.* **2000**, *39*, 2360.

were calculated taking loss of ligands into account. Infrared spectra were recorded on a Mattson Polaris Fourier transform spectrometer with 2 cm^{-1} resolution. All solution IR spectra were recorded at the highest concentration that allowed all bands to be nicely resolved (i.e., the most intense peak reaching nearly zero transmittance). With the cell path length 0.1 mm, this concentration is estimated to be $(1-3) \times 10^{-3}$ M.

X-ray Structure Determination. From the X-ray studies, it was found that all of the structures possess disordered THF molecules, as well as disordered Mn in **1**, disordered CO in **1**, **2**, and **4,** and disordered Et_2O in **3**. The recognition of disorder was based on the suggestion in SHELX97 of its possibility for an atom if U1, the largest of its principal thermal ellipsoid axes, is greater than 0.2 $Å^2$ and if U1 is more than 2.5 times as large as its second largest such axis. For THF, the splitting was extended over the C atoms, and the occupancies were estimated using PART 1 and PART 2 options in SHELX97. The temperature factors are large, and only isotropic temperature factors were used in these disordered regions. In addition, THF molecules that lie close to the 2-fold axis in **6** were assigned occupancies of 0.5. All but two of these atoms were refined anisotropically. DFIX restraints were applied to atoms in the disordered regions: Mn−O (1.81 Å), C−C (1.52 Å), C−O (1.43 Å) for THF and C−O (1.13 Å) for CO, all with esd = 0.02 Å. The ordered regions of the structures were not seriously affected by various changes in the models of the disordered regions, and their bond distances and angles values appear to be reliable although they have larger than desirable esd's. The latter effect seems to be the result of the very heavy atoms (many electrons) present which contribute most of the X-ray scattering as well as to the disorder.

Single crystals of compounds **1**−**6** were grown using the slow evaporation of solvent technique and kept in their mother liquor until just before they were mounted on the X-ray diffractometer. Compound **2** was difficult to crystallize, and our best attempts only led to crystals of relatively low quality. Single-crystal X-ray diffraction data were collected using graphite-monochromated Mo Kα radiation ($\lambda = 0.71073$ C) on a Nonius KappaCCD diffraction system. Single crystals of **1**−**6** were mounted on the tip of a glass fiber coated with Fomblin oil (a perfluoropolyether) that provided protection from the atmospheric oxygen. Crystallographic data were collected at 200 K for all compounds. Unit cell parameters were obtained by indexing the peaks in the first 10 frames and were refined employing the whole data set. All frames were integrated and corrected for Lorentz and polarization effects using the Denzo-SMN package (Nonius BV, 1999).[34] Absorption corrections were applied to structures **1**, **3**, **5**, and **6** using the SORTAV program[35] provided by MaXus software.[36] Absorption corrections for structures **2** and **4** were accounted for by using SCALEPACK. All of the structures were solved by direct methods and refined using the SHELXTL-97 (difference electron-density calculation, full matrix least-squares refinements) structure solution package, and some other programs.[37] For each structure, all the non-hydrogen atoms were located and refined anisotropically with the exception of the carbon atoms of the Et_2O and THF ligands in **3** that were refined isotropically. Hydrogen atoms on solvent ligands were calculated assuming standard geometries.

Preparation of $[Yb(L)_n][M(CO)_5]_2$, 1, 1a, 1b, 1c, and 2. The syntheses of these compounds are all similar (except for **2**) and will be given here using $[Yb(THF)_6][Mn(CO)_5]_2$ as an example. Note that single crystals and X-ray analyses were obtained for compounds **1** and **2** only. There are two routes for preparation of **1**, **1a**, **1b**, and **1c**: (a) via $Hg[M(CO)_5]_2$[38] and (b) via ytterbium amalgam. Compound **2** could only be prepared using route a; preparation of **2** via route b was attempted several times and failed repeatedly.

Route a. A 50 mL flask was charged with 296 mg (0.5 mmol) of $Hg[Mn(CO)_5]_2$ and 87 mg (0.5 mmol) of Yb. Approximately 20 mL of THF was condensed into the flask at −78 °C. The mixture was warmed to room temperature and stirred overnight, during which time the solution became dark red and Hg appeared. Infrared spectroscopy was used to monitor the reaction. Filtration of the reaction mixture through Celite gave a dark-red filtrate. Dark-red chunklike crystals appeared in 1 day after slow evaporation of the solvent at room temperature until 3 mL of solution remained. It was found that to obtain the best X-ray quality crystals, the initially crystallized material should be left in the mother liquor for about a week at room temperature. The mother liquor was then removed, and the crystals were washed with 3 mL of THF and 10 mL of hexanes. The crystals were dried under vacuum for 5 min, yielding 338 mg of **1** (68% yield based on $Hg[Mn(CO)_5]_2$). Anal. Calcd for $YbMn_2C_{26}H_{32}O_{14}$ (−2 THF): C, 36.7; H, 3.80. Found: C, 36.25; H, 3.90. For **2**, the yield was somewhat lower (340 mg, 54% based on $Hg[Re(CO)_5]_2$). For **1c**, Anal. Calcd for $YbMn_2C_{30}H_{20}O_{10}N_4$ (−2 pyr): C, 40.9; H, 2.29. Found: C, 39.6; H, 2.68. For **2**, Anal. Calcd for $YbRe_2C_{18.8}H_{17.6}O_{12.2}$ (−3.8 THF): C, 22.94; H, 1.81. Found: C, 22.56; H, 2.00.

Route b. A 50 mL flask was charged with ytterbium amalgam prepared from ∼5 mL of Hg, 95 mg (0.55 mmol) of Yb, and 195 mg (0.5 mmol) of $Mn_2(CO)_{10}$. Approximately 20 mL of THF was condensed into the flask at −78 °C. The mixture was warmed to room temperature and stirred overnight, during which time the solution became dark red. Subsequent treatment of the solution led to a crop of crystals that were the same as those obtained from route a. Yield of **1**: 358 mg (72% based on $Mn_2(CO)_{10}$).

Preparation of $\{(THF)_2(Et_2O)_2Yb[(\mu\text{-}(CO)_2Mn(CO)_3)_2]\}_\infty$, 3. In a 50 mL flask, compound **1** was prepared from 118 mg (0.20 mmol) of $Hg[Mn(CO)_5]_2$ and 35 mg (0.20 mmol) of Yb. The THF solvent was removed under vacuum, and ∼30 mL of Et_2O was condensed into the flask at −78 °C. The mixture was warmed to room temperature and stirred overnight, during which time the solution became green. Filtration of the reaction mixture through Celite gave a green filtrate. Emerald-green crystals of **3** appear immediately when evaporation of the solvent begins. Good X-ray quality material can be obtained at an evaporation rate of ∼3.5−4 mL/h. Yield: 57 mg (33% based on $Hg[Mn(CO)_5]_2$). Dry crystals of **3** lose coordinated Et_2O easily. Anal. Calcd for $YbMn_2C_{18}H_{16}O_{12}$ (−2Et_2O): C, 30.6; H, 2.28. Found: C, 30.4; H, 2.69.

Preparation of $\{(THF)_4Yb[(\mu\text{-}CO)_2Mn(CO)_3)_2]\}_\infty$, 4. In a 50 mL flask, compound **1** was prepared from 591 mg (1.0 mmol) of $Hg[Mn(CO)_5]_2$ and 173 mg (1.0 mmol) of Yb. The THF solvent was removed under vacuum, and ∼35 mL of Et_2O was condensed into the flask at −78 °C. The mixture was warmed to room temperature and stirred overnight, during which time the solution became green. Filtration of the reaction mixture through Celite gave a green filtrate. The filtrate was allowed to remain in the flask for

(34) Otwinowski, Z.; Minor, W. In *Methods in Enzymology*; Carter, C. W., Jr., Sweet, R. M., Eds.; Academy Press: New York 1997; Vol. 276A, p 307.
(35) Blessing, R. H. *J. Appl. Crystallogr.* **1997**, *30*, 421.
(36) Mackay, S.; Gilmore, C. J.; Edwards, C.; Tremayne, M.; Stuart, N.; Shankland, K. *MaXus*; University of Glasgow: Glasgow, Scotland; Nonius BV: Delft, The Netherlands; and MacScience Co., Ltd.: Yokohama, Japan, 1998.
(37) (a) Sheldrick, G. M. *SHELXTL-97*; University of Göttingen: Göttingen, Germany, 1998. (b) *WinGX*, version 1.70.01. Farrugia, L. G. *J. Appl. Crystallogr.* **1999**, *32*, 837−838.
(38) Hsieh, A. T. T.; Mays, M. J. *J. Chem. Soc. A* **1971**, 2648.

3 days, during which time its color changed from green to yellow. Dark Yb precipitate formed on the bottom of the flask, and crystals of **4** began to appear on the flask's walls. The Et_2O solvent was then evaporated in the course of 4 more days until ∼3 mL of it remained, producing well-shaped yellow crystals of **4** stuck to the walls. The remaining solvent was pipetted out, and the crystals were carefully collected with a spatula. Yield: 238 mg (28% based on $Hg[Mn(CO)_5]_2$). Anal. Calcd for $YbMn_2C_{18}H_{16}O_{12}$ (−2 THF): C, 30.6; H, 2.26. Found: C, 28.9; H, 2.81.

Preparation of $(THF)_2Mn_3(CO)_{10}$, 5. A 50 mL flask containing crystals of **4** and ∼2 mL of the mother liquor was allowed to remain for 5 days, during which time the material in the flask started to turn from yellow to red. Investigation under a microscope revealed that yellow crystals of **4** were mixed with some ruby-red crystals, that were identified as compound **5**. All subsequent attempts to repeat this preparation led either to the formation of **6**, or they did not yield results. For this reason, no analyses except the X-ray structure determination were performed on this compound.

Preparation of $[(THF)_5Yb(\mu\text{-}CO)Mn_3(CO)_{13}][Mn_3(CO)_{14}]$, 6. Crystals of **4** and ∼2 mL of the mother liquor was allowed to remain for 7 days in a 50 mL flask, at the end of which period large, needle-shaped ruby-red crystals of **6** formed. The only way crystals of **6** could be separated from the remaining crystals of **4** was by means of hand-picking them, since both **4** and **6** are soluble and insoluble in the same solvents. The amount of the material formed never exceeded 4 crystals at a time. This and the difficulty of a clean reproduction of the synthesis prevented us from performing analyses other than the X-ray diffraction on this compound.

Acknowledgment. This work was supported by the National Science Fondation through Grant CHE 02-13491.

Supporting Information Available: Detailed X-ray structural data including a summary of crystallographic parameters, atomic coordinates, bond distances and angles, anisotropic thermal parameters, and H atom coordinates for structures **1**−**6**, and the IR spectra of compounds **1**, **1a**, **1b**, **1c**, **2**−**4**. This material is available free of charge via the Internet at http://pubs.acs.org.

IC060756K